International Journal of Computing and Digital Systems
2025, VOL. 17, NO. 1, 1–15

http://dx.doi.org/10.12785/ijcds/1571020535

GPR Signal Processing for Landmine Detection: A Comparative Study of Feature Extraction and Classification Algorithms

T. Kalaichelvi[1] **and S. Ravi**[2]

[1,2]*Computer Science, Pondicherry University, Puducherry, India*

Received 18 April 2024, Revised 9 October 2024, Accepted 5 December 2024

Abstract: Landmine detection faces a significant challenge in identifying buried explosives that complicate efforts to ensure the safety of affected areas. These buried explosives substantially threaten human lives, hindering economic growth and development efforts. Traditional methods for landmine detection often need to be revised, as they rely on time-consuming manual techniques and cannot identify non-metallic landmines. Fortunately, Advancements in technology offer various methods for locating buried landmines. Ground penetrating radar (GPR) has emerged as a powerful tool for subsurface exploration, emitting electromagnetic waves and recording reflections to create an image of buried objects. However, GPR data presents a complex image containing reflections and clutters from underground utilities besides landmines, complicating the detection process. Effective detection of landmines relies on successfully separating the target signals of landmines from background clutter and noise. This paper presents a comparative study of feature extraction and classification techniques for GPR-based landmine detection. The initial stage involves feature extraction, where the algorithms identify key characteristics within the GPR data that discriminate landmines from other objects. Various feature extraction approaches are discussed, including image processing techniques such as edge detection through the Scharr and Sobel operator, spatial, and spectral features retrieval, and many statistical methods for analyzing signal intensity variations. Classification algorithms, including support vector machine (SVM) and k-nearest neighbors (K-NN), can effectively learn and classify discriminatory features from labeled GPR datasets containing landmines. This paper evaluates and compares the effectiveness of various feature extraction and classification algorithms using performance metrics such as the probability of detection (Pd), accuracy, and false alarm rate (FAR).

Keywords: Buried Object, Classification, Clutter, Feature Extraction, Ground Penetrating Radar, Landmine Detection.

1. Introduction

Landmines remain a significant global threat to human safety, hindering economic growth and impeding development efforts. These explosive devices are buried under the ground and detonated upon contact with a person, vehicle, animal, or pressure [1]. The blast of a mine can cause direct and indirect damage through explosive force and shrapnel. Beyond immediate casualties, landmines also have a lasting impact, disrupting agricultural land use and harming the environment [2].

Effective landmine detection is a complex task influenced by various factors. However, the performance of each technique varies depending on the type of explosive used, the landmine shape, the properties of the soil, and the materials used in its construction [3]. Researchers employ surrogate or simulated landmines and non-mine objects generated through gprMax software [4] buried at various depths and sizes during data collection and some researchers used experimental and real-world data.

Many countries around the world face a life-threatening danger from landmines. It is estimated that 80 countries remain affected by landmine contamination. These hidden explosives claim a devastating toll each year, with casualties ranging from 15,000 to 25,000 people killed or maimed [5]. About 80% of casualties by landmines are civilians, particularly children. Landmine Monitor 2020 [6] emphasizes the urgent need to remove landmines to ensure the safety of affected communities, facilitate the return of displaced populations, and support post-conflict recovery and development efforts. Figure 1 shows the landmine contamination status for 2020. Many countries have adopted the global ban on landmines, and international funding supports demining operations. The Ottawa Treaty enforces the AP landmine ban convention, mandating landmine clearance by 2025 [7].

E-mail address: assertivekalai@gmail.com, sravicite@pondiuni.ac.in

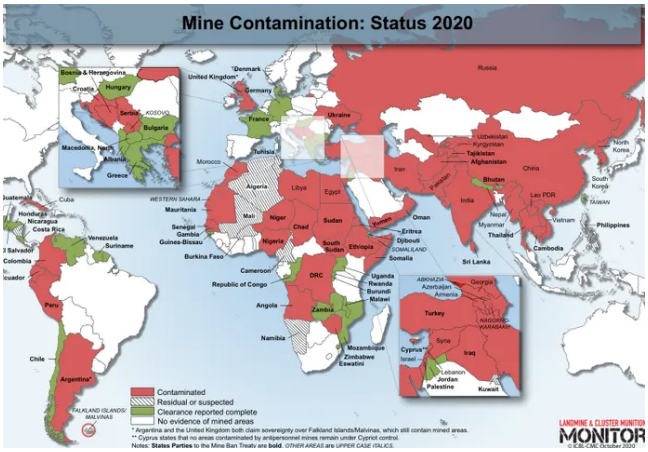

Figure 1. Mine Contamination Status Report 2020 [6]

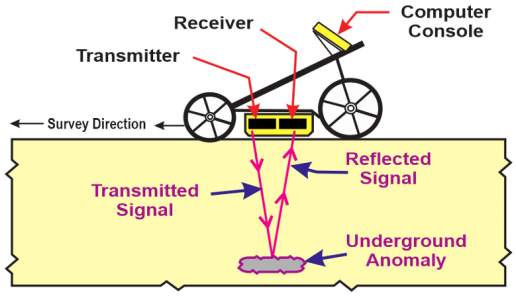

Figure 2. Process of Ground Penetrating Radar [8]

Landmine detection and demining are inherently challenging, time-consuming, and often dangerous. Fortunately, advances in sensor technology, image processing, and machine learning are providing promising solutions to detect landmines. GPR is a valuable tool for landmine detection and also detects other buried utilities. It uses electromagnetic (EM) signals to image objects buried beneath the ground surface. The transmitter antenna sends the EM wave towards the object, and the receiver antenna records the reflected energy. Differences in the electromagnetic properties of subsurface objects cause anomalies in the received signal. The software then processes these anomalies to generate an image. Figure 2 illustrates the entire process of ground-penetrating radar involved in landmine detection [8]. GPR has built-in memory to store data at the end of the examination. It is a non-invasive subsurface sensing method to detect landmines made of metal, non-metal, and plastic.

Significant research focuses on automating landmine detection using GPR data. However, challenges arise due to clutter in the image data caused by surface scattering, target interaction, and variations in the subsurface. Fortunately, various algorithms and techniques can distinguish between landmines and clutter based on their specific characteristics. These methods extract features from GPR images to determine the presence or absence of landmines. Soil composition can significantly impact the effectiveness of GPR-based landmine detection methods. These methods underscore the ongoing challenges in this field and the needed improvement in various detection techniques. An overview and comparison of GPR-based landmine detection technologies are presented.

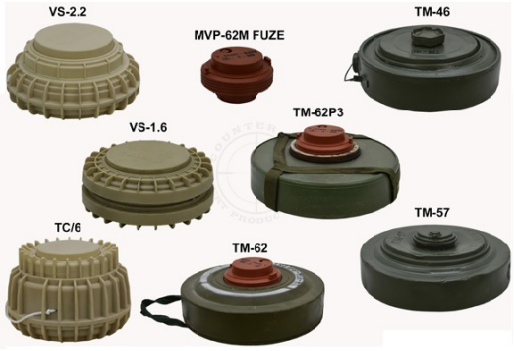

Figure 3. Types of Anti-Tank Landmines [9]

Section 1 introduces landmines and provides the current state of landmine detection. Section 2 categorizes landmines and explains the demining process. Section 3 analyzes the various explosive detection techniques for identifying buried objects. Section 4 reviews landmine detection methods utilizing GPR technology. Section 5 compares the different feature extraction and classification algorithms used for landmine detection based on GPR techniques. The comparison also discusses the corresponding advantages, limitations, datasets involved, and performance metrics achieved. Finally, section 6 summarizes findings and future research directions.

2. Categories of Landmines and Demining

A. *Types of Landmines*

Landmines come in two distinct categories: Anti-Tank (AT) and Anti-Personnel (AP). AT landmines, also known as anti-vehicular landmines, typically have cylindrical or square shapes ranging from 150-300 mm in diameter and 50-90 mm in thickness. It contains powerful explosives such as TNT, Composition B, or RDX [5]. It comes in various shapes and sizes, including metal, plastic, or wood casings material used for landmines to make them difficult to detect. They detonate when subjected to a minimum pressure of 200 kilograms, typically triggered by vehicles driving over them. These landmines, primarily used on battlefields, are designed to destroy tanks and trucks. These weapons can cause casualties for people inside and around the targeted vehicle, posing a significant threat to civilians caught in conflict zones. Figure 3 showcases various anti-tank landmines [9].

In contrast to AT landmines, AP landmines target only individuals. These disc-shaped devices are compact, typically measuring 20-125 mm in diameter, 50-100 mm in length, and weighing 30 grams. Common explosives used in AP landmines include TNT, Tetryl, and Comp B [5].

Figure 4. Types of Anti-Personnel Landmines [10]

Detonation occurs under pressure as low as 2 kilograms or when someone steps on the mine. Figure 4 provides the various anti-personnel landmine products [10]. There are two main subcategories of AP landmines: blast and fragmentation mines [11].

Unexploded ordnance (UXO), which are explosive devices that failed to detonate as intended [12]. The rise of improvised landmines further complicates detection efforts and increases civilian casualties. Landmine-triggering mechanisms vary considerably, including pressure-based activation systems, electronic triggers, remote detonation, light or sound sensitivity, and magnetic influences.

B. Types of Demining Methods

Landmines can remain active over five decades, necessitating demining efforts to prevent casualties. Demining refers to removing landmines from contaminated areas. Two primary methods exist for demining process are military and humanitarian demining.

1) Military Demining

The military demining method prioritizes speed over the complete removal of landmines. It employs a brute force approach, utilizing vehicles to clear paths through minefields. Despite achieving an estimated 80% clearance rate, it accepts a certain level of casualties and leaves behind a significant portion of landmines.

2) Humanitarian Demining

A more intricate and meticulous process is humanitarian demining, which focuses on the safe and complete removal of landmines with minimal environmental impact. It aims for a near-perfect 99.6% clearance rate. However, this safer method comes at a higher cost per landmine removal. It exposes deminers to risk, with an estimated one fatality for every 2,000 landmines clearance [5] [13].

3. Explosive Detection

Researchers have explored various landmine detection techniques such as biological, electromagnetic, acoustic, mechanical, optical, and nuclear.

A. Biological Detection

Biological detection techniques utilize trained animals such as rats, dogs, insects like bees, and ants alongside plants and bacteria to sense the presence of explosive materials. This type of sensor detects landmines, but their effectiveness depends on various factors. Table I compares biological sensor's requirements, performance, and problems.

B. Electromagnetic Detection

The electromagnetic detection method identifies variations in the electromagnetic properties of buried objects compared to the surrounding ground surface. The transmitter emits signals within a specific frequency range, and the receiver interprets the reflected signals to detect anomalies. Table II shows the various electromagnetic sensor's requirements, performance, and problems.

C. Acoustic Detection

Acoustic sensors project acoustic waves toward the ground. These waves reflect off the materials they encounter, depending on the acoustic properties of those materials, which can cause vibrations due to their mechanical characteristics. Table III presents the acoustic detection techniques, outlining their requirements, performance, and problems.

D. Mechanical Detection

Mechanical detection of landmines utilizes physical interaction with the ground to locate buried explosives by machines and probes. Table IV details mechanical detection techniques with requirements, performance, and problems.

E. Optical Detection

It penetrates the optical wave to buried materials and measures the soil surface property. Table V displays the optical detection techniques with requirements, performance, and problems.

F. Nuclear Detection

The standard nuclear detection technique is nuclear quadrupole resonance (NQR), which uses radio-frequency and neutron-based techniques. Table VI reports nuclear detection techniques with requirements, performance, and problems.

Landmine detection remains a complex task due to limitations in current technologies. Both metal detectors (MD) and GPR are widely used for the identification of landmines, and each has advantages and disadvantages. Techniques like Bacterial and NQR show promising results with low false alarm rates, but widespread adoption might be limited. MDs are prone to false alarms when encountering even small amounts of metal debris.

Ideally, a landmine detection system should be efficient, accurate, and have a minimal false alarm rate. Unfortunately, no single sensor or method can guarantee complete detection across all scenarios. Several factors hinder landmine identification, including obstacles such as rocks or vegetation, the presence of metallic debris, variations in temperature and humidity, and different types of soil composition. Therefore, multiple sensor usage is crucial to

TABLE I. Biological sensors requirements, performance, and problems

Sensors	Requirements	Performance	Problems
Rats [11]	Food reward training to locate explosives	Increased detection rate with more numbers of rats	Susceptible to tropical diseases
Dogs [14]	Extensive training in explosives	High success rate for detecting explosives	Mood, time, and behavioral variations
Plants [15]	Genetically modified plants need a controlled environment	Detect the presence of nitrogen dioxide	Prone to false alarms
Ants [16]	No training is required, can self-deactivate	Capable of locating explosives back to the nest	Limited range and detection capabilities
Bacteria [17]	A genetically modified bacteria sprayed in the field	Covers large areas and detects TNT	Highly sensitive, leading to false positives
Bees [18]	Trained to associate a chemical odor with food reward	Effective at detecting landmines	Limited operation range due to temperature restrictions

TABLE II. Electromagnetic sensors requirements, performance, and problems

Sensors	Requirements	Performance	Problems
Metal Detector [19]	Measure the reflected current induced by the field	Prone to false alarms; Cannot detect a non-metallic object	Difficult to detect in highly conductive soils
Ground Penetrating Radar [20]	Transmit and receives radio waves to detect reflected signals	Effective for metallic and non-metallic objects detection	Inconsistent in homogeneous soil
Microwave Radar [21]	Transmit microwaves and analyze reflected signals	Detect small and large objects	Performance can be slow in wet soil conditions
Millimeter-Wave Radar [22]	Send millimeter wave and collect reflected radiation	Penetrate on obstacles like clouds, smoke, and dry soil	Challenges faced across varying soil conditions
Electrical Impedance Tomography [23]	Measure current to map underground properties	Suitable for wet soil and detect all types of objects	Background noise that can hamper performance
X-ray Backscatter [24]	Pass x-ray photons and analyze	Effective for shallowly buried objects	Difficult to detect deep objects
Infrared [25]	Detect variations in temperature and light properties	Detect non-metallic landmines	Ineffective to detect deep objects

TABLE III. Acoustic sensors requirements, performance, and problems

Sensors	Requirements	Performance	Problems
Ultrasound [26]	Sound waves emitted by acoustic sensors and reflect off the ground	Propagate in wet areas and underwater	Not efficient in sand
Acoustic to Seismic [27]	Generates acoustic or seismic waves and analyzes the vibration based on mechanical properties	Detect both types of landmines and gives low false alarm rates	Detection speed is slow

TABLE IV. Mechanical detection requirements, performance, and problems

Sensors	Requirements	Performance	Problems
Clearing Machines [13]	Machines are rolling in the field to clear the path	Take a short time to remove landmine	Trigger landmine when the use of heavy-sized machines
Prodder and Probes [28] [29]	Scan shallow area at a 30-degree angle	Identify the unusual object based on sound	Explode when prodding, become hazardous

TABLE V. Optical sensors requirements, performance, and problems

Sensors	Requirements	Performance	Problems
LIDAR [10]	Identifies the polarization changes in the backscattered energy	Detect metallic and non-metallic objects and covers large areas	Highly vegetated areas are not suitable
Light [12] [13]	Capturing light waves from the object	A large area scanned only on flat land in a shorter time	Less effective in poor lighting conditions

TABLE VI. Nuclear detection requirements, performance, and problems

Sensors	Requirements	Performance	Problems
Nuclear Quadrupole Resonance [30]	Used radio frequency and identify nitrogen atom nuclei in TNT	Effective in the detection of TNT or RDX explosive	Identify landmines with a strong signal
Nuclear Magnetic Resonance [31]	Used along with a metal detector	Detect nitrogen present in TNT	Detect only landmine objects placed inside the coil

enhance the accuracy and reliability of landmine detection. These sensors collect diverse data to aid in the exact identification of landmines. GPR, in particular, offers a variety of feature extraction and classification techniques. GPR can analyze these features to identify buried landmines through proven classification algorithms.

4. Review of Feature Extraction and Classification Methods used for Landmine Detection

Bhuiyan and Nath [32] used a seeded region growing segmentation (SRGS) to extract features and classify them through a feed-forward neural network (FFNN). The input x_j mentioned in Equation (1) is given to the neural network (NN), and to produce output y from Equation (2) which identified the pattern as a landmine or not, where n is the length of the pattern and f as activation function. w_i, and w_{ij} denoted the weight connected to the output and the hidden layer neuron. Figure 5 shows the SRGS-oriented feature extraction and FFNN as classification.

$$x_j = I(j) \tag{1}$$

$$y = \int \left(\sum_{i=1}^{m} w_i f_i \sum_{j=1}^{n} w_{ij} x_j \right) \tag{2}$$

Z. Ma compared the Hidden Markov Model (HMM), edge histogram descriptors (EHD), spectral correlation feature (SCF), and Geometric (GEOM) discrimination methodologies to recognize landmines and clutter objects using vehicle-mounted GPR [33]. Using EHD, H. Frigui and P. Gader extracted translation-invariant features from the identified regions of interest (ROI). Then, a probabilistic K-NN is used to determine the confidence value $Conf(S_T)$ mentioned in Equation (5) based on the mine $Conf^{(M)}(S_T)$ Equation (3), and the clutter $Conf^{(C)}(S_T)$ Equation (4) classes for accurate detection [34].

$$Conf^{(M)}(S_T) = \frac{1}{K} \sum_{k=1}^{K} \left(\tilde{\mu}^M(R_k) \cdot w^{(p)}(S_T, R_k) \right) \tag{3}$$

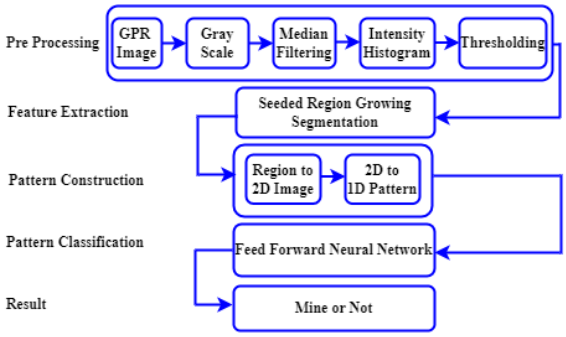

Figure 5. Seeded Region Growing Segmentation and Feed Forward Neural Network Architecture [32]

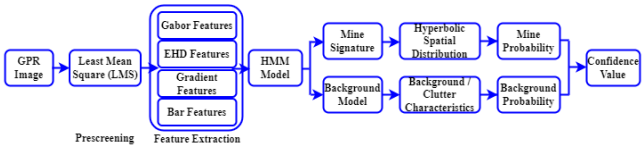

Figure 6. Hidden Markov Model for Discrimination of Landmine and Clutter Signatures [35]

$$Conf^{(C)}(S_T) = \frac{1}{K} \sum_{k=1}^{K} \left(\tilde{\mu}^C(R_k) \cdot w^{(p)}(S_T, R_k) \right) \tag{4}$$

$$Conf(S_T) = \sqrt{Conf^{(M)}(S_T) \times \left(1 - Conf^{(C)}(S_T)\right)} \tag{5}$$

HMM was proven to be an effective technique used for landmine detection based on GPR data. This framework extracted the gradient features from GPR signatures. K-NN classifier and bar histogram used EHD to retrieve the features of buried objects. Figure 6 shows the HMM for discrimination of landmine and clutter signatures [35]. A supervised learning model retrieved spectral features of identified ROI by using the least mean square (LMS). Equation (6) normalizes the magnitude of Fourier-transformed

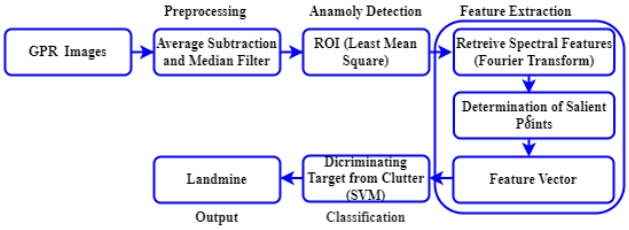

Figure 7. Feature Extraction and Classification using Fourier Transform and Support Vector Machine [36]

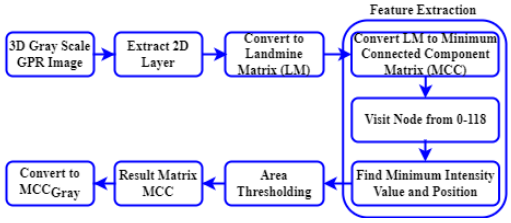

Figure 8. Minimum Connected Component-based Feature Extraction for Landmine Detection [37]

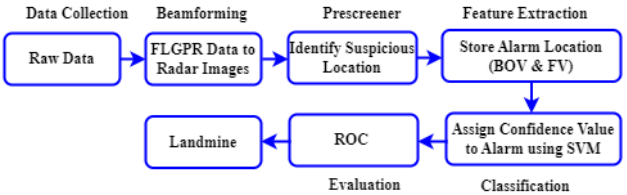

Figure 9. Feature Learning approach using Bag of Visual Words and Fisher Vector [38]

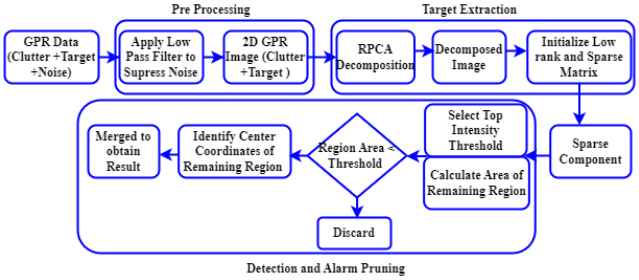

Figure 10. Robust Principal Component Analysis-Go Decomposition based Feature Extraction and Detection [39]

data (P_k) to reduce its dependency on soil losses. A. Dyana et al. base this normalization on the N-point discrete Fourier transformed data ($|S_k|$), and frequency (k). Figure 7 displays Fourier Transform (FT) for feature extraction and SVM' for classification process [36].

$$P_k = \frac{|S_k|}{\sum_{k=0}^{N-1} |S[k]|/N} \tag{6}$$

Ramasamy et al. proposed a minimum connected component (MCC) based on graph theory to identify covered objects from 2D GPR images. Figure 8 illustrates the conversion process from landmine matrix to MCC and MCC_{Gray} [37]. Camilo et al. used the bag of visual words (BOV) and fisher vector (FV) as feature-learning approaches for forward-looking GPR data processing. Based on the background mean μ and standard deviation σ, the normalized feature (X') was extracted from image X using Equation (7).

$$X' = \frac{|X| - \mu_{bg}}{\sigma_{bg}} \tag{7}$$

The final BOV and FV features were retrieved using equations (8) and (9) based on the dimensionality of raw and scale-invariant feature transform (SIFT) descriptors intensities under various soil conditions. Figure 9 shows the feature learning approach for feature extraction using BOV and FV [38].

$$\psi_{BOV}(X \mid D) = \left\{ \max_t \gamma_t(k) \; ; \; k = 1, \ldots, K \right\} \tag{8}$$

$$\psi_{FV}(X \mid u_\lambda) = \{ g^X_{\mu_k} \; g^X_{\sigma_k} \; ; \; k = 1, \ldots, K \} \tag{9}$$

Song et al. proposed robust principal component analysis (RPCA) to prescreen AP mine (APM) from GPR images and employed GoDecomposition (GoDec) to retrieve the target. Figure 10 displays the RPCA-GoDec feature extraction and landmine identification process [39]. Yuan et al. developed the twin gray statistics sequence (TGSS) to classify GPR features using row and column vectors of a B-scan image. This method involves calculating the twin gray sequence from the image's gray statistics level h defined using Equations (10) and (11), utilizing a gray-level co-occurrence matrix (GLCM) for classification. Figure 11 illustrates the feature classification process using TGSS [40].

$$u_i(h) = \frac{1}{N} \sum_{y=1}^{N} \delta(G(i, y) = e_h) \tag{10}$$

$$v_i(h) = \frac{1}{M} \sum_{x=1}^{M} \delta(G(x, y) = e_h) \tag{11}$$

Harkat et al. proposed a multi-objective genetic algorithm (MOGA) for classification. The MOGA classifier used features retrieved using higher-order statistics (HOS) and mutual information feature selection (MIFS). Figure 12 details the classification process involving the multi-objective genetic algorithms [41]. Mesecan et al. calculated feature on row and column indices using Equations (12) and (13) for the data x and derived the final feature vector (FV) using Equation 14, as shown in Figure 13 [42].

$$Feature_c = \sqrt{\sum_{r=2}^{Rows} \left(x_{rc} - x_{(r-1)c}\right)^2} \tag{12}$$

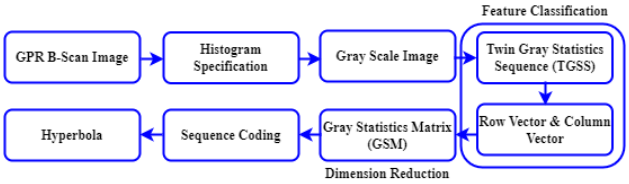

Figure 11. Feature classification using Twin Gray Statistics Sequence [40]

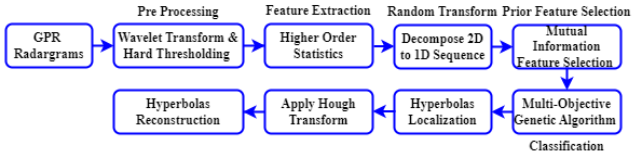

Figure 12. Process of Classification through Multi-Objective Genetic Algorithm [41]

$$Feature_r = \sqrt{\sum_{c=2}^{Cols} \left(x_{rc} - x_{r(c-1)}\right)^2} \tag{13}$$

$$FV_{rc} = [Feature_r, Feature_c] \tag{14}$$

N. Smitha and V. Singh extracted three and five features from GPR images and classified them via SVM and NN. Figure 14 displays three and five features of feature extraction with a neural network classifier [43].

A. Gharamohammadi and A. Shokouhmand calculated a correlation coefficient between the scattering parameter and the whitening algorithm to detect the anomaly. The RPCA observed the data matrix X using Equation (15) from low-rank component G, sparse component S, and noise N [44].

$$X = G + S + N \tag{15}$$

Figure 13. Feature Vector for Underground Object Detection from GprMax [42]

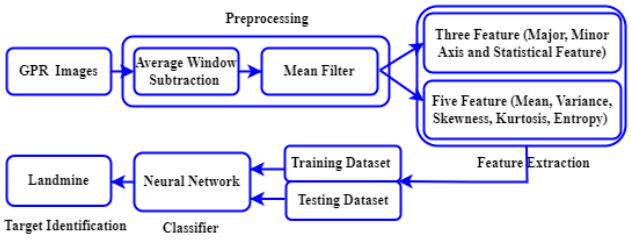

Figure 14. Five Features of Feature Extraction with Neural Network Classifier [43]

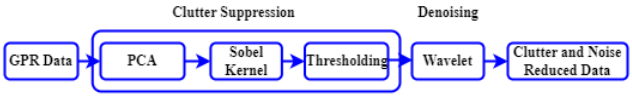

Figure 15. Gradient-Based Clutter Suppression and Wavelet-Based Denoising [47]

The initial low-rank matrix G_0 and the sparse matrix S_0 calculated using Equations (16) and (17) based on data matrix X and transposition vector T.

$$G_0 = \left(\frac{1}{N}\sum_{i=1}^{N} x_i\right)\mathbf{1}^T_{(N\times 1)} \tag{16}$$

$$S_0 = X - G_0 \tag{17}$$

J. F. Lozano et al. proposed an intelligent multi-agent system using various sensors. Each agent operates independently to optimize data acquisition and local decision-making (LDM), sharing information with other agents. The final decision arises on collaborative details in the cooperative decision-making (CDM) system. Features are calculated for visible spectrum (VS), infrared (IR), and ultraviolet (UV) sensors using Equation (18) [45].

$$\Gamma = [\Lambda, \lambda, \mu, \sigma_M, \xi, K, \zeta, \rho, \epsilon, \phi] \tag{18}$$

A. D. Pambudi proposed a likelihood-ratio test (LRT) using FLGPR [46] to construct a band of feasible probability densities for each hypothesis. B. S. Kumar et al. employed gradient magnitude with thresholding to remove unwanted clutters and utilized wavelet-based denoising to eliminate noise from the GPR images. The approach measured the peak signal-to-noise ratio (PSNR) using Equation (19) based on mean square error (MSE) and image entropy (IE) using Equation (20). Figure 15 displays the process of clutter suppression and denoised data for classification [47].

$$PSNR(dB) = 10\log_{10}\left(\frac{L^2}{MSE}\right) \tag{19}$$

$$H = \frac{\left(\sum_{m=0}^{M-1}\sum_{n=0}^{N-1} B^2(m,n)\right)^2}{\sum_{m=0}^{M-1}\sum_{n=0}^{N-1} B^4(m,n)} \tag{20}$$

P. Bestagini et al. analyzed the framework trained on GPR data captured in landmine-free areas using autoencoders. It used different polarizations to analyze GPR images but required improvement in localizing the anomaly [48]. M.M. Omwenga et al. proposed an autonomous cognitive GPR (AC-GPR) using deep reinforcement learning (DRL) with a reward system for detecting ROI and classifying objects. Deep Q-learning networks (DQNs) were created to handle dimensionality issues in state space and help the system learn effective policies [49]. F.M. El-Ghamry et al. presented the Gauss gradient and speeded up robust feature (SURF) descriptor method. Gauss gradient

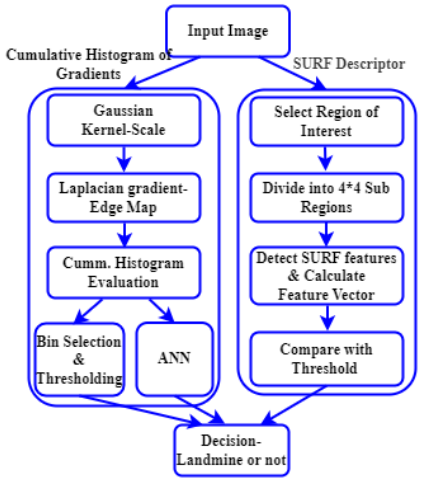

Figure 16. Feature Extraction using Cumulative Histogram of Oriented Gradients and SURF Descriptor [50]

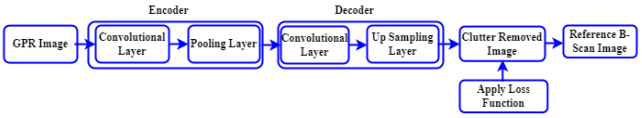

Figure 17. Convolutional Auto-Encoder Architecture to Remove Clutter [51]

algorithm estimated the cumulative HOG using Equation (21) using the image details D_{fx} and D_{fy}. SURF detector identified the feature vector v using Equation (22) from the 4x4 sub-region in horizontal direction d_x and vertical direction d_y.

$$D_{fxy} = |D_{fx}| + |D_{fy}| \tag{21}$$

$$v = \left[\sum d_x, \sum |d_x|, \sum d_y, \sum |d_y|\right] \tag{22}$$

Figure 16 illustrates the feature extraction based on HOG and SURF descriptor for landmine detection [50].

The convolutional auto-encoder (CAE) removed clutter from images, directly highlighting target components. Its filter coefficients depended on the kernel size and the number of filters in both the encoder and decoder. The signal-to-clutter ratio (SCR) measured the CAE's effectiveness on actual data. Figure 17 displays the CAE architecture to remove clutter from the GPR image [51]. M. N. Motafram et al. used a CNN to extract information from B-scans and an RNN to model differential data and retrieve features from cross and down-track scans [52]. M.G. Fernandez et al. [53] enhanced the airborne GPR systems to detect landmines by addressing issues of height information and antenna tilt.

N. Barkataki et al. [54] presented a CNN model to predict the size of buried objects based on edge detection techniques using the Sobel and Scharr operator to preprocess the GPR B-Scans images. H. Zhou et al. [55] introduced a particle center AdaBoost (PCAD) method of improved target classification in full-polarimetric ground-penetrating radar (FPGPR), enhancing the identification of underground objects as landmines. F. Xie et al. [56] enhanced the GPR tool by modeling uncertainty in target depth before and after surveys, finding that uncertainty increases with depth on pre-survey. In contrast, post-survey uncertainty is influenced by reflection data noise. S. Ghanbari et al. [57] improved subsurface utility detection by employing a data acquisition and processing strategy that includes compensated time reversal (CTR) techniques.

M. Elbadry et al. [58] utilized a finite element (FE) framework to study the coupled electromagnetic and mechanical behavior of buried targets, using the Lorentz force of mechanical equations. H. Liu et al. [59] used the You Only Look Once version 3 (YOLOv3) model to identify pipelines under the subsurface. The iterative threshold transformed the hyperbolic response into a binary image to determine a buried pipeline position and depth. Y. Su et al. [60] used key point–regression mode to retrieve the ROI and hyperbola. N. Barkataki et al. [61] proposed an artificial neural network (ANN) to detect the size of buried objects from GPR A-Scan images with a minimum mean absolute percentage error (MAPE) of 1.89%. Y. Yu and C.C. Chen [62] classified UXO components using entropy-based polarimetric features. A. Afrasiabi et al. [63] presented a Kalman Filter (KF)-with a MOGA optimization algorithm for GPR that reduces noise and improves the detection of buried utilities with less user input.

F. Cui et al. [64] introduced a multi-polarization GPR array that uses multiple antenna dual-field domain-decomposition time-domain finite-element methods (DFDD-TDFEM) to enhance detection resolution and data acquisition. N. Q. Hoang et al. [65] employed SwinIR, RCAN, and MSRN combinations to improve the quality of GPR images to find the anomaly with an excellent structural similarity index (SSIM) measure and an enhanced anomaly detection in GPR images using a novel loss function that combines cross-entropy and reconstruction loss [66]. G. Junkai et al. [67] presented GPR-TransUNet, an inversion network of deep learning for GPR that utilizes a self-attention mechanism and regression techniques.

5. Comparison of Gpr Sensors Data with Feature Extraction and Classification

Table VII compares GPR data processed through various algorithms to identify specific features for landmine classification. Each technique has its advantages and limitations, and the data used for implementation reflects accuracy (Acc), probability of detection, and false alarm rate.

A. Feature Extraction Methods

Landmine detection is crucial to distinguish landmines and non-mines from their surroundings when they have distinct shapes and sizes. Various feature extraction methods were used to retrieve features from B-Scan images of landmines generated through gprMax. Spectral feature retrieval is employed in [33] and [36] to identify the ROI from

TABLE VII. Comparison of GPR sensor data with an algorithm, features, advantages, limitations, dataset, and performance metrics

Algorithm	Features	Advantages	Limitations	Dataset	Metrics
Median Filtering, SRGS, FFNN [32], 2006	Region-Based	Efficient and reliable for accurately detecting and classifying AP mines	Tested on a small amount of actual data	DeTeC at the EPFL	Pd-80%
HMM, GEOM, SCF, EHD [33], 2007	Edge, Geom, Spectral	HMM delivered the best performance on the data collected	HMM algorithms take longer times to process each alarm than EHD	NIITEK data	Pd-90%, FAR-0.002
EHD, KNN [34], 2009	Edge	Fuzzy techniques distinguished false alarms from accurate detection	Factors appear to be influenced by geography and the environment	NIITEK data	Pd - 90%
HMM [35], 2012	Gradient, Gabor, Bar, Edge	Histogram detected 13 types of AT landmines	EHD was less effective than other algorithms	NIITEK data	Pd-95% (EHD), FAR-0.0118
SVM [36], 2017	Spectral	Performed better for landmine detection than edge and gradient features	Multiple features can enhance classification accuracy	Real-world data	Acc-0.83
MCC [37], 2017	High-Intensity Edges	Efficient landmine detection was achieved using grayscale images	The effectiveness of feature extraction alone was not a major factor in detection	Grayscale landmine image	Confidence Level-95%
SVM, SIFT Descriptor [38], 2017	BOV, FV	Performed well with BOV and FV methods applied to images in HH polarization	Feature learning did not perform well for other feature sets in all polarizations	Western US Army Data	FAR-0.02
RPCA-GoDec [39], 2018	Sparse Component	GoDec with thresholds offered fast computation and robustness against clutter and noise	Target discrimination had to be focused more	Georgia Technology Institute	Pd- 99%
TGSS [40], 2019	Twin Feature	Performed well in dimension reduction	Accuracy rate varied when changes in the training data	Real data	Acc-82.77%
MOGA [41], 2019	HOS	MOGA performed well on the training set and showed strong results on the validation and testing data	Design time was longer than neural networks but faster than SVM	Maas and Schmalzl Data	Acc-91.03%
KNN, SVM, HOG [42], 2019	Gradient	HOG produced better results when KNN used	Reduced the noise level in signals	Synthetic Data	Average Performance-92.6%
SVM and NN Classifier [43], 2020	Five Feature Set	NN method outperformed SVM	Did not include different soil types and moisture	Surrogate Data	Acc (NN - 95%)
Whitening Algorithm [44], 2020	S-Parameter	ZCA-correlation whitening algorithm performed well on the simulated database	The simulation did not consider soil inhomogeneity	Georgia Tech	Correlation Coefficient-89.74%
CDM [45], 2020	LDM and CDM	The system detected IEDs of any shape, material, and type	GPR, TS performed worse than VS, showing improvement only in CDM	Fabio Caraffini Data	Acc-0.7778 (IR)
LRT in Density Band and Outlier [46], 2020	Feasible probability density	Reduced false alarms and missed detections in a robust outlier	Hypothesis test is necessary to properly assess the accuracy of the LRT	US Army	FA-8, MD-2
PCA, Wavelet denoising [47], 2021	Gradient	Performed well in clutter suppression, PSNR, and entropy in a homogeneous medium	Testing in heterogeneous soil and rough surface conditions is essential	Synthetic and measured	PSNR-37.28, IE-698.4
Autoencoder [48], 2021	Multi-polarization	Horizontal and vertical polarization achieved better accuracy	Autoencoder enabled only a limited amount of data	Real data	Acc - 93%

TABLE VII. Comparison of GPR sensor data with an algorithm, features, advantages, limitations, dataset, and performance metrics (Continued)

Algorithm	Features	Advantages	Limitations	Dataset	Metrics
DRL [49], 2021	DQN	Performed well in object detection and classification accuracy	Worked only in a homogeneous environment	Simulated (gprMax)	Classification-$7.12X10^3$
Cumulative HOG, SURF Descriptor [50], 2022	Gradient and SURF	SURF achieved a higher Pd with no false alarms than Gaussian gradients	Interpolation restored the original image after decimation reduced its size	Real data	Acc-89%
CAE, DCAE [51], 2022	Texture	Effectively removed clutters and provided the simulated target	Performed slightly worse on real data compared to LRSD-based methods	Vrije Universite Brussel	Clutter-0.119(CAE), 0.197(DCAE)
CNN-RNN [52], 2022	LSTM	Feature extracted using both CNN and RNN	Possible only when using deep learning algorithms	Real	Pd-0.9
Distance-based SVD filtering [53], 2022	Extract Height Information	Different radar angles improve GPR-SAR image focus and reduce clutter	Co-registration must to compensate the different antenna tilt	GPR-SAR images	Detection-100%
Deep CNN [54], 2022	Scharr operator	The Scharr operator with the CNN yielded the best results	Successful training requires many images	Simulated (gprMax)	MAPE-6.74
PCAD [55], 2022	FP-GPR	Selected optimal parameters with higher classification accuracy	Multiple parameters have been used	Laboratory	Acc-87.8%
Uncertainty [56], 2022	Scattering noise	Improving reliability in engineering applications	Estimated only depth	IFSTTAR	Confidence interval-95%
CTR [57], 2022	Kirchhoff migration	Offered better resolution and higher signal-to-noise	Location identified by drilling	Simulated	Precise utility location
FE Framework [58], 2022	Lorentz Force	Detected buried object in heterogeneous medium	Permittivity was not considered	Simulated	Target depth
R-CNN [59], 2023	YOLOv3	YOLOv3 recognized the regions of the pipeline	Took longer to divide the image into areas of interest	Real	Precision-95.6%
End-End DL [60], 2023	Key point regression	Support good accuracy and maintain operating speed	Parameters cannot be optimized with deep learning	Real and simulated	Acc-97.01%
Deep Learning [61], 2023	ANN	Exact features retrieved through several layers of neurons	Highest errors occurred for non-metallic targets with smaller diameter values	Real Data	MAPE-1.89%
Scattering [62], 2023	Entropy-Based	Fully polarimetric radar data used	Need to determine the best features	US UXO test site	ROC Curve
MOGA [63], 2023	KF	More efficient approach to GPR data processing	Semi-autonomous nature	DZT GGSI	Acc-91.4%
DFDD-TDFEM [64], 2023	Signal aggregation	System improves signal quality	Only concentrated on Quality of images	Simulated	Improved signal-to-noise ratio
Ensemble Network [65], 2024	SwinIR, RCAN, MSRN	Reduces misclassification and improves classification accuracy	Not suitable for blurred GPR images	Simulated	SSIM-0.980
ViT [66], 2024	Cross-entropy	Background and white noise enhances detection performance	Weighted factor used between 0 to 10 only	Simulated	Acc-92.5%
TransUNet [67], 2024	Self-attention	Superior performance in training stability and inversion accuracy	Computational Complexity	Simulated and Guangxi	Permittivity inversion

GPR B-Scan images. Translation-invariant features were used to get the edge of the landmine within an image in [34], [35], and [37] based on edge histogram descriptors. The gradient method was used in [35], [36], [42], [47], and [50], while various feature sets have been employed, including the twin feature set in [40], the two feature sets in [38], and the five feature sets in [43]. Statistical feature extraction methods were selected for their ability to quantify image properties such as texture and intensity distributions [51], making them helpful in distinguishing between types of objects and backgrounds based on variations in soil and landmine features. The above methods were chosen because they provide the most essential features of landmines and their surroundings.

B. Classification Algorithms

The classification algorithms were chosen based on the nature of the feature data extracted. SVM and K-NN are used for classification when there is complex feature space and high-dimensional data with non-linear decision boundaries. The SVM method is employed in [36], [38], [41], [42], and [43] because of its robustness in the usage margin between classes. K-NN is selected for multiclass problems in [42].

C. GPR Datasets

Developing robust landmine detection and analysis models requires variation in characteristics. The GPR datasets vary in characteristics, including the type of casing material, metallic and non-metallic, soil type, shape, size, orientation, depth penetration, environmental conditions, scan dimensions, and number of scan traces. Some datasets may include high-resolution subsurface scans, while others may have a lower resolution but cover a larger area. The datasets were divided into three subsets for evaluating machine learning algorithms: training, validation, and testing.

D. Incorporation of Deep Learning

CNNs' ability to handle complex image data and automatically extract features may offer considerable advantages in landmine detection. The paper discusses and compares these advanced techniques involved in normalization, resizing, and data augmentation. The study would present a more thorough analysis and demonstrate the potential for improved detection performance. Deep learning techniques employed in [49], [52], [54], [59], [60], [61], and [67] are helpful for feature extraction from GPR B-Scan images because they can learn hierarchical features automatically. The architectures range from simple to complex, utilizing varying convolutional layers, such as ResNet and U-Net, based on the dataset's size and complexity. CNNs are adept at adapting to a wide range of features and patterns present in GPR images, which can significantly enhance the accuracy of landmine detection compared to traditional methods like SVM and K-NN.

E. Evaluation of Computational Efficiency

Deep learning shows varying levels of complexity, which scale with the number of layers and the size of the kernels. Training CNN requires GPUs or specialized hardware resources, and to enhance processing speed for real-time applications, optimized libraries and hardware accelerators can be employed. Furthermore, optimization techniques commonly utilized for SVM and K-NN, such as dimensionality reduction, parallel processing, and efficient data structures, can enhance computational efficiency. Several strategies are used for CNNs, including quantization, pruning, and lightweight architectures like EfficientNet and MobileNet, to reduce computation load. Together, these approaches make deep learning models more effective for real-time applications.

F. Comparison with Baseline Models

As per the study, Traditional baseline models in GPR-based landmine detection include statistical, spectral [33], edge detection [33], [34], [35], [37] and [54], gradient [35], [42], [47] and [50], and machine learning classifiers features to learn landmine signatures from GPR B-Scan images. Deep learning methods might include advanced machine learning approaches such as ensemble methods [62].

G. Ablation Study

Evaluate the performance of feature extraction methods using only edge detection without statistical features; it understands the impact of edge-based features alone on detection accuracy. However, statistical methods without edge detection isolate the effect of statistical features on the overall performance.

The performance of SVM compared to other classification algorithms, such as random forest, decision trees, or gradient boosting machines, evaluates how different classifiers impact detection accuracy and robustness. Similarly, the performance of K-NN with alternative classifiers will be compared to determine its relative effectiveness.

The authors [33], [35], [50], and [62] have compared the results with other feature extraction techniques and compared the performance based on evaluation metrics such as accuracy, precision, recall, F1 score, and probability detection.

H. False Alarm Rate

FAR measures underground objects incorrectly identified as landmines. According to the comparative study, a lower FAR is essential for reliable landmine detection, as false positives can lead to unnecessary disruptions and risks. Techniques such as feature selection, classifier optimization, and post-processing filtering are utilized to minimize FAR. Ensemble methods like bagging and boosting can enhance performance by leveraging the strengths of multiple algorithms, reducing FAR while improving Pd.

There is often a trade-off between Pd and FAR. Increasing Pd typically requires lowering the detection threshold, which can raise FAR due to more false positives. Conversely, reducing FAR may necessitate a higher threshold, potentially lowering Pd.

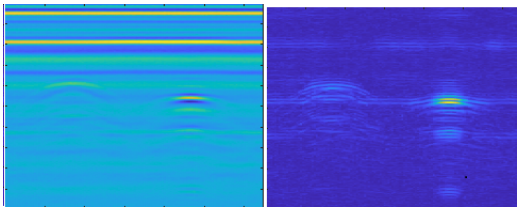

Figure 18. Images before and after applying Gradient Magnitude [47]

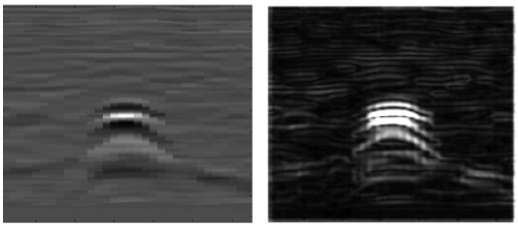

Figure 19. Images before and after applying the Gauss gradient [50]

SVM can be adjusted using different kernels and regularization parameters to balance Pd and FAR, whereas, in K-NN, the number of neighbors and distance metrics influence this trade-off. Various thresholds and architecture adjustments can be used to adjust deep learning models.

I. Visualization

Visualization includes the input and output of GPR B-scan images before and after applying algorithms to reduce clutter and extract landmine-related features. Figure 18 displays the images before and after applying Gradient Magnitude [47]. Figure 19 shows the images before and after applying the Gauss Gradient to retrieve features of landmines GPR B-Scan images [50].

J. Limitations

The performance and limitations of the algorithms are presented in Table VII. The data availability is crucial for landmine detection, serving as the foundation for training and evaluating detection algorithms. It may vary by technique, soil type, and depth of burial. However, specific algorithms may perform better in dry, sandy soils than in clay or loamy soils based on differences in EM wave propagation and attenuation. Environmental factors such as moisture content, temperature, and the presence of other subsurface materials can also affect algorithm performance and introduce noise or distortions in GPR signals; the depth of the buried objects can significantly impact signal quality and accuracy.

K. Findings

This study compared feature extraction and classification algorithms for landmine detection using GPR data, aimed to identify the most effective approach to maximize detection probability while minimizing false alarms. The analysis revealed that clutter on GPR data, caused by buried objects and soil variations, significantly hinders accurate landmine identification. Several researchers explored many clutter reduction algorithms, like SURF descriptors [50], Sobel and Scharr operator for pre-processing [54], and machine learning features such as two [38] and five-feature sets [43], BOV, FV [38], and CAE [51] parameters involved to mitigate the challenges. These techniques were designed to retrieve salient features and reduce clutter, eventually enhancing detection accuracy.

In addition, the study evaluated the performance of several classification algorithms, including SVM [36], [38], [42], and [43], NN [43], KNN [34], and [42], and FFNN [32], to distinguish landmines from non-mines. In this context, spectral feature-based classifiers, especially SVMs, performed better than NN classifiers using gradient and edge features. These findings underscore the critical role of effective clutter reduction and feature extraction in GPR-based landmine detection. The promising performance of SVM classifiers highlights their potential for real-world applications.

6. Conclusion and Future Work

This paper presents the challenges faced by various landmine detection techniques. Particularly, GPR offers a promising solution due to its non-invasive nature and ability to detect subsurface objects. However, the complexity of GPR data necessitates robust feature extraction and classification techniques to distinguish landmine signatures from clutter and noise effectively. This study also highlights the comparative performance of various feature extraction methods, such as edge detection and statistical methods, alongside classification algorithms like SVM and K-NN. Continued technological advancements and interdisciplinary collaboration will be essential for improving landmine detection systems and ensuring safety in affected regions. However, some researchers concentrate on specific aspects, such as clutter reduction, feature extraction, or classification. Effective landmine detection requires a multifaceted approach that integrates pre-processing, clutter reduction, feature extraction, and classification methods.

In the future, Researchers should focus on deep learning techniques for clutter reduction, feature extraction, and classification of GPR data, including CNNs, which have shown considerable promise in signal processing tasks. Developing deep learning models tailored to GPR signal characteristics can enhance robustness against varying soil conditions and signal noise, paving the way for more effective landmine detection solutions.

References

[1] UNMAS, “Landmines, explosive remnants of war and ied safety handbook,” 2015, https://unmas.org/sites/default/files/handbook_english.pdf.

[2] Minesweepers, “About Minesweepers - Minesweepers — landmine-free.org,” 2021, https://landminefree.org/about.

[3] ICBL, "Landmine and cluster munition monitor — monitor," 2009, http://archives.the-monitor.org/index.php/publications/display?url=lm/2013/sub/Mine_Action.html.

[4] C. Warren, A. Giannopoulos, and I. Giannakis, "gprmax: Open source software to simulate electromagnetic wave propagation for ground penetrating radar," *Computer Physics Communications*, vol. 209, pp. 163–170, 2016, https://doi.org/10.1016/j.cpc.2016.08.020.

[5] E. Hussein and E. Waller, "Landmine detection: the problem and the challenge," *Applied Radiation and Isotopes*, vol. 53, no. 4, pp. 557–563, 2000, https://doi.org/10.1016/S0969-8043(00)00218-9.

[6] Reliefweb, "Mine contamination: Status 2020," 2020, https://reliefweb.int/map/world/mine-contamination-status-2020.

[7] C. Loughran and C. Wallen, "Landmine free 2025," 2018, https://themimu.info/sites/themimu.info/files/documents/Core_Doc_Policy_Brief_-_The_Ottawa_Treatys_2025_goal_for_clearance.pdf.

[8] U. G. U. Locating, "Ground penetrating radar logo, ground penetrating radar for finding unmarked graves," https://ug-locating.com/gpr.

[9] Inert, "Anti-Tank Landmines," 2024, https://inertproducts.com/product/inert-anti-tank-landmine-kit.

[10] Inert, "Anti-personnel landmines," 2024, https://inertproducts.com/product/inert-anti-personnel-landmine-kit.

[11] H. Kasban, O. Zahran, S. Elaraby, M. Kordy, and F. Abd El-Samie, "A comparative study of landmine detection techniques," *Sensing and Imaging*, vol. 11, pp. 89–112, 2010, https://doi.org/10.1007/s11220-010-0054-x.

[12] USArmy, "Unexploded ordnance (uxo): An overview october 1996," 1996, https://apps.dtic.mil/sti/pdfs/ADA422504.pdf.

[13] P. C. Bhope and A. S. Bhalchandra, "Various landmine detection techniques: A review," *International Journal of Innovative Research in Science, Engineering and Technology*, vol. 4, 2015, https://www.ijirset.com/upload/2015/multicon/ece/60_EC087.pdf.

[14] P. A. Prada and M. C. Rodrguez, "Demining dogs in colombia – a review of operational challenges, chemical perspectives, and practical implications," *Science Justice*, vol. 56, pp. 269–277, 2016, https://doi.org/10.1016/j.scijus.2016.03.002.

[15] M. K. Habib, "Controlled biological and biomimetic systems for landmine detection," *Biosensors and Bioelectronics*, vol. 23, pp. 1–18, 2007, https://doi.org/10.1016/j.bios.2007.05.005.

[16] J. E. McFee, S. Achal, A. A. Faust, E. Puckrin, A. House, D. Reynolds, W. McDougall, and A. Asquini, "Detection and dispersal of explosives by ants," *Detection and Sensing of Mines, Explosive Objects, and Obscured Targets XIV*, 2009, https://doi.org/10.1117/12.820232.

[17] R. Liu, Z. Li, Z. Huang, K. Li, and Y. Lv, "Biosensors for explosives: State of art and future trends," *TrAC Trends in Analytical Chemistry*, vol. 23, 2019, https://doi.org/10.1016/j.trac.2019.05.034.

[18] T. Wasilewski, J. Gebicki, and W. Kamysz, "Bio-inspired approaches for explosives detection," *TrAC Trends in Analytical Chemistry*, vol. 142, 2021, https://doi.org/10.1016/j.trac.2021.116330.

[19] S. Masunaga and K. Nonami, "Controlled metal detector mounted on mine detection robot," *International Journal of Advanced Robotic Systems*, 2007, https://doi.org/10.5772/5692.

[20] H. P. Kazunori Takahashi and J. Igel, "Soil properties and performance of landmine detection by metal detector and ground-penetrating radar — soil characterisation and its verification by a field test," *Journal of Applied Geophysics*, vol. 73, pp. 368–377, 2011, https://doi.org/10.1016/j.jappgeo.2011.02.008.

[21] D. S. Kailash Chandra Tiwari and M. Arora, "Development of a model for detection and estimation of depth of shallow buried non-metallic landmine at microwave x-band frequency," *Progress in Electromagnetics Research*, vol. 79, pp. 225–250, 2008, https://doi.org/10.2528/PIER07100201.

[22] T. W. D. Bosq, J. M. Lopez-Alonso, G. D. Boreman, D. Muh, J. Grantham, and D. Dillery, "Millimeter wave imaging system for the detection of nonmetallic objects," *Detection and Remediation Technologies for Mines and Minelike Targets XI*, 2006, https://doi.org/10.1117/12.665607.

[23] S. G. Philip Church, John E. Mcfee and P. Wort, "Electrical impedance tomographic imaging of buried landmines," *IEEE Transactions on Geoscience and Remote Sensing*, vol. 44, pp. 2407–2420, 2006, https://doi.org/10.1109/TGRS.2006.873208.

[24] G. J. Lockwood, S. L. Shope, L. B. Bishop, M. M. Selph, and J. Jojola, "Mine detection using backscattered x-ray imaging of antitank and antipersonnel mines," *Proceedings of the SPIE*, vol. 3079, pp. 408–417, 1997, https://doi.org/10.1117/12.280915.

[25] B. Nelson, "Region of interest identification, feature extraction, and information fusion in a forward looking infrared sensor used in landmine detection," *Proceedings IEEE Workshop on Computer Vision Beyond the Visible Spectrum: Methods and Applications*, pp. 94–103, 2000, https://doi.org/10.1109/CVBVS.2000.855254.

[26] C. Bruschini and B. Gros, "A survey of research on sensor technology for landmine detection," *The Journal of Humanitarian Demining*, vol. 2, 1998, http://commons.lib.jmu.edu/cisr-journal/vol2/iss1/3.

[27] N. Xiang and J. M. Sabatier, "An experimental study on antipersonnel landmine detection using acoustic-to-seismic coupling," *The Journal of the Acoustical Society of America*, vol. 113 3, pp. 1333–41, 2003, https://api.semanticscholar.org/CorpusID:22773364.

[28] C. P. Gooneratne, S. Mukhopahyay, and G. Gupta, "A review of sensing technologies for landmine detection : Unmanned vehicle based approach," *2nd International Conference on Autonomous Robots and Agents*, 2004, https://api.semanticscholar.org/CorpusID:34308663.

[29] J. Macdonald, J. Lockwood, J. Mcfee, T. Altshuler, T. Broach, L. Carin, R. Harmon, C. Rappaport, W. Scott, and R. Weaver, *Alternatives for Landmine Detection*. RAND, 2003, https://www.rand.org/pubs/monograph_reports/MR1608.html.

[30] Y. Tan, S. Tantum, and L. Collins, *Landmine detection with nuclear quadrupole resonance*. IEEE International Geoscience and Remote Sensing Symposium, 2002, vol. 3, https://doi.org/10.1109/IGARSS.2002.1026185.

[31] L. Cardona, H. Itozaki, J. Jiménez, N. Vanegas, and H. Sato-Akaba, "Design of a radio-frequency transceiver coil for landmine detection in colombia by nuclear quadrupole resonance," *Heliyon*, vol. 6, p. e03242, 2020, https://doi.org/10.1016/j.heliyon.2020.e03242.

[32] A. Bhuiyan and B. Nath, "Anti-personnel mine detection and classification using gpr image," in *18th International Conference on Pattern Recognition (ICPR'06)*, vol. 2, 2006, pp. 1082–1085, https://doi.org/10.1109/ICPR.2006.274.

[33] Z. Ma, "Advanced feature based techniques for landmine detection using ground penetrating radar," *Thesis*, 2007, https://doi.org/10.32469/10355/4971.

[34] H. Frigui and P. Gader, "Detection and discrimination of land mines in ground-penetrating radar based on edge histogram descriptors and a possibilistic *k*-nearest neighbor classifier," *IEEE Transactions on Fuzzy Systems*, vol. 17, no. 1, pp. 185–199, 2009, https://doi.org/10.1109/TFUZZ.2008.2005249.

[35] A. Hamdi and H. Frigui, "Evaluation of various feature extraction methods for landmine detection using hidden markov models," *Proc. SPIE, Detection and Sensing of Mines, Explosive Objects, and Obscured Targets XVII*, vol. 8357, 2012, https://doi.org/10.1117/12.924086.

[36] A. Dyana, S. Vadada, C. H. S. Rao, and S. Gorthi, "Landmine discrimination using spectral features from ground penetrating radar data," in *International Conference on Radar Systems (Radar 2017)*, 2017, pp. 1–4, https://doi.org/10.1049/cp.2017.0450.

[37] V. Ramasamy, D. Nandagopal, M. Tran, and C. Abeynayake, "A novel feature extraction algorithm for ied detection from 2-d images using minimum connected components," *Procedia Computer Science*, vol. 114, pp. 507–514, 2017, https://doi.org/10.1016/j.procs.2017.09.018.

[38] J. A. Camilo, L. M. Collins, and J. M. Malof, "A large comparison of feature-based approaches for buried target classification in forward-looking ground-penetrating radar," *IEEE Transactions on Geoscience and Remote Sensing*, vol. 56, pp. 547–558, 2018, https://doi.org/10.1109/TGRS.2017.2751461.

[39] X. Song, D. Xiang, K. Zhou, and Y. Su, "Fast prescreening for gpr antipersonnel mine detection via go decomposition," *IEEE Geoscience and Remote Sensing Letters*, vol. 16, pp. 15–19, 2019, https://doi.org/10.1109/LGRS.2018.2866331.

[40] D. Yuan, Z. An, and F. Zhao, "Gray-statistics-based twin feature extraction for hyperbola classification in ground penetrating radar images," *Procedia Computer Science*, vol. 147, pp. 567–573, 2019, https://doi.org/10.1016/j.procs.2019.01.215.

[41] H. Harkat, A. Ruano, M. Ruano, and S. Bennani, "Gpr target detection using a neural network classifier designed by a multi-objective genetic algorithm," *Applied Soft Computing*, vol. 79, pp. 310–325, 2019, https://doi.org/10.1016/j.asoc.2019.03.030.

[42] I. Mesecan, B. Cico, and I. O. Bucak, "Feature vector for underground object detection using b-scan images from gprmax," *Microprocessors and Microsystems*, vol. 76, p. 103116, 2020, https://doi.org/10.1016/j.micpro.2020.103116.

[43] N. Smitha and V. Singh, "Target detection using supervised machine learning algorithms for gpr data," *Sens Imaging*, vol. 21, pp. 1–15, 2020, https://doi.org/10.1007/s11220-020-0273-8.

[44] A. Gharamohammadi and A. Shokouhmand, "A robust whitening algorithm to identify buried objects with similar attributes in correlation-based detection," *Journal of Applied Geophysics*, vol. 172, p. 103917, 2020, https://doi.org/10.1016/j.jappgeo.2019.103917.

[45] J. Florez-Lozano, F. Caraffini, C. Parra, and M. Gongora, "Cooperative and distributed decision-making in a multi-agent perception system for improvised land mines detection," *Information Fusion*, vol. 64, pp. 32–49, 2020, https://doi.org/10.1016/j.inffus.2020.06.009.

[46] A. D. Pambudi, M. Fauß, F. Ahmad, and A. M. Zoubir, "Minimax robust landmine detection using forward-looking ground-penetrating radar," *IEEE Transactions on Geoscience and Remote Sensing*, vol. 58, pp. 5032–5041, 2020, https://doi.org/10.1109/TGRS.2020.2971956.

[47] B. S. Kumar, A. K. Sahoo, and S. Maiti, "Removal of clutter and random noise for gpr images," in *2021 IEEE 18th India Council International Conference (INDICON)*, 2021, pp. 1–6, https://doi.org/10.1109/INDICON52576.2021.9691520.

[48] P. Bestagini, F. Lombardi, M. Lualdi, F. Picetti, and S. Tubaro, "Landmine detection using autoencoders on multipolarization gpr volumetric data," *IEEE Transactions on Geoscience and Remote Sensing*, vol. 59, pp. 182–195, 2021, https://doi.org/10.1109/TGRS.2020.2984951.

[49] M. M. Omwenga, D. Wu, Y. Liang, L. Yang, D. Huston, and T. Xia, "Cognitive gpr for subsurface object detection based on deep reinforcement learning," *IEEE Internet of Things Journal*, vol. 8, pp. 11 594–11 606, 2021, https://doi.org/10.1109/JIOT.2021.3059281.

[50] F. M. El-Ghamry, W. El-Shafai, M. I. Abdalla, G. M. El-Banby, A. D. Algarni, M. I. Dessouky, A. S. Elfishawy, F. E. A. El-Samie, and N. F. Soliman, "Gauss gradient and surf features for landmine detection from gpr images," *Computers, Materials, and Continua*, vol. 71, pp. 4457–4487, 2022, https://doi.org/10.32604/cmc.2022.022328.

[51] E. Temlioglu and I. Erer, "A novel convolutional autoencoder-based clutter removal method for buried threat detection in ground-penetrating radar," *IEEE Transactions on Geoscience and Remote Sensing*, vol. 60, pp. 1–13, 2022, https://doi.org/10.1109/TGRS.2021.3098122.

[52] M. N. Motafram, S. V. Athawale, A. Padhye, P. Kulkarni, and N. Pawar, "Advanced buried threat detection using convolutional neural networks and recurrent neural networks," *SAMRIDDHI : A Journal of Physical Sciences, Engineering and Technology*, vol. 14, pp. 416–420, 2023, https://smsjournals.com/index.php/SAMRIDDHI/article/view/3040.

[53] M. Garcia-Fernandez, G. Álvarez Narciandi, Y. Álvarez Lopez, and F. L.-H. Andres, "Improvements in gpr-sar imaging focusing and detection capabilities of uav-mounted gpr systems," *ISPRS Journal of Photogrammetry and Remote Sensing*, vol. 189, pp. 128–142, 2022, https://doi.org/10.1016/j.isprsjprs.2022.04.014.

[54] N. Barkataki, B. Tiru, and U. Sarma, "A cnn model for predicting size of buried objects from gpr b-scans," *Journal of Applied Geophysics*, vol. 200, p. 104620, 2022, https://doi.org/10.1016/j.jappgeo.2022.104620.

[55] H. Zhou, X. Feng, Z. Dong, C. Liu, and W. Liang, "Multiparameter adaptive target classification using full-polarimetric gpr: A novel approach to landmine detection," *IEEE Journal of Selected Topics in Applied Earth Observations and Remote Sensing*, vol. 15, pp. 2592–2606, 2022, https://doi.org/10.1109/JSTARS.2022.3159305.

[56] F. Xie, W. W. Lai, and X. Dérobert, "Building simplified uncertainty models of object depth measurement by ground penetrating radar,"

Tunnelling and Underground Space Technology, vol. 123, p. 104402, 2022, https://doi.org/10.1016/j.tust.2022.104402.

[57] S. Ghanbari, M. K. Hafizi, M. Bano, A. Ebrahimi, and N. Hosseinzadeh, "An enhanced gpr-based data processing approach for detecting subsurface utilities in urban distribution networks," *Journal of Applied Geophysics*, vol. 207, p. 104831, 2022, https://doi.org/10.1016/j.jappgeo.2022.104831.

[58] M. Elbadry, J. Wetherington, and M. Zikry, "Coupled electromagnetic and mechanical modeling and detection of buried objects," *Applications in Engineering Science*, vol. 10, p. 100106, 2022, https://doi.org/10.1016/j.apples.2022.100106.

[59] H. Liu, Y. Yue, C. Liu, B. Spencer, and J. Cui, "Automatic recognition and localization of underground pipelines in gpr b-scans using a deep learning model," *Tunnelling and Underground Space Technology*, vol. 134, p. 104861, 2023, https://doi.org/10.1016/j.tust.2022.104861.

[60] Y. Su, J. Wang, D. Li, X. Wang, L. Hu, Y. Yao, and Y. Kang, "End-to-end deep learning model for underground utilities localization using gpr," *Automation in Construction*, vol. 149, p. 104776, 2023, https://doi.org/10.1016/j.autcon.2023.104776.

[61] N. Barkataki, B. Tiru, and U. Sarma, "Size estimation of underground targets from gpr frequency spectra: A deep learning approach," *Journal of Applied Geophysics*, vol. 213, p. 105009, 2023, https://doi.org/10.1016/j.jappgeo.2023.105009.

[62] Y. Yu and C.-C. Chen, "Automatic subsurface unexploded ordnance detection using a wideband full-polarization ground penetrating radar and entropy-based polarimetric signatures," *Journal of Applied Geophysics*, vol. 209, p. 104913, 2023, https://doi.org/10.1016/j.jappgeo.2022.104913.

[63] A. Afrasiabi, A. Faramarzi, D. Chapman, A. Keshavarzi, and M. Stringfellow, "Toward the optimisation of the kalman filter approach in ground penetrating radar application for detection and locating buried utilities," *Journal of Applied Geophysics*, vol. 219, p. 105220, 2023, https://doi.org/10.1016/j.jappgeo.2023.105220.

[64] F. Cui, G. Dong, Y. Chen, C. Wang, D. Teng, and R. Wang, "Numerical modeling and data signal analysis of gpr array based on dual-field domain-decomposition time-domain finite element method," *Journal of Applied Geophysics*, vol. 208, p. 104876, 2023, https://doi.org/10.1016/j.jappgeo.2022.104876.

[65] N. Q. Hoang, S. Shim, S. Kang, and J.-S. Lee, "Anomaly detection via improvement of gpr image quality using ensemble restoration networks," *Automation in Construction*, vol. 165, p. 105552, 2024, https://doi.org/10.1016/j.autcon.2024.105552.

[66] N. Q. Hoang, S. Kang, H.-K. Yoon, and J.-S. Lee, "Enhancing anomaly detection in ground-penetrating radar images through reconstruction loss and high-variability," *Results in Engineering*, vol. 21, p. 101874, 2024, https://doi.org/10.1016/j.rineng.2024.101874.

[67] G. Junkai, S. Huaifeng, S. Wei, L. Dong, Y. Yuhong, Z. Yi, L. Rui, and L. Shangbin, "Gpr-transunet: An improved transunet based on self-attention mechanism for ground penetrating radar inversion," *Journal of Applied Geophysics*, vol. 222, p. 105333, 2024, https://doi.org/10.1016/j.jappgeo.2024.105333.